DEPARTMENT OF MECHANICAL ENGINEERING
COLLEGE OF ENGINEERING & TECHNOLOGY
OLD DOMINION UNIVERSITY
NORFOLK, VIRGINIA 23529

THE EFFECTS OF PROFILES ON SUPERSONIC JET NOISE

By

T.R.S. Bhat, Research Associate

and

S.N. Tiwari, Principal Investigator

Progress Report
For the period ended January 31, 1994

Prepared for
National Aeronautics and Space Administration
Langley Research Center
Hampton, VA 23681-0001

Under
Research Grant NAG-1-1581
Dr. John M. Seiner, Technical Monitor
ACOD- Aeroacoustic Branch

Submitted by the
Old Dominion University Research Foundation
P.O. Box 6369
Norfolk, Virginia 23508-0369

February 1994

FOREWORD

This is a semi-annual progress report on the research project, "Instability Wave Models and Supersonic Jet Noise", for the period August 1993 - January 1994. The funding for this research was provided by the NASA Langley Research Center through the Grant NAG-1-1518. The grant was monitored by Dr. John M. Seiner of Aeroacoustics Branch (Acoustics Division), Mail Stop 165, NASA Langley Research Center, Hampton, VA 23681.

THE EFFECT OF VELOCITY PROFILES ON SUPERSONIC JET NOISE

T. R. S. Bhat† and S. N. Tiwari§
Department of Mechanical Engineering
Old Dominion University, Norfolk, VA 23529-0247

ABSTRACT

The effect of velocity profiles on supersonic jet noise are studied by using stability calculations made for a shock-free coannular jet, with both the inner and outer flows supersonic. The Mach wave emission process is modeled as the noise generated by the large scale turbulent structures or the instability waves in the mixing region. Both the vortex-sheet and the realistic finite thickness shear layer models are considered. The stability calculations have been performed for both inverted and normal velocity profiles. Comparisons are made with the results for an equivalent single jet, based on equal thrust, mass flow rate and exit area to that of the coannular jet. The advantages and disadvantages of these velocity profiles as far as noise radiation is concerned are discussed. It is shown that the Rayleigh's model prediction of the merits and demerits of different velocity profiles are in good agreement with the experimental data.

---

† Research Associate
§ Eminent Professor

TABLE OF CONTENTS

LIST OF FIGURES

LIST OF SYMBOLS

A_n, B_n	Unknown coefficients
b	Half-width of the shear layer
C	Speed of sound
C_n, D_n	Unknown coefficients
C_δ	Shear layer spread coefficient
f	Frequency in cycles/sec
h	Radius of the core region
H_n	Hankel function of the first kind of order n
J_n	Bessel's function of the first kind of order n
M	Mach number
M_R	Convective Mach number
n	Azimuthal mode number
p	Perturbation pressure
$\hat{p}$	Pressure eigenfunction
(r, θ, x)	Cylindrical coordinate system
R	Radius
St	Strouhal number, $2fR_i/U_i$
T	Mean temperature
U	Mean axial velocity
Y_n	Bessel's function of the second kind of order n

Greek Symbols

α	Axial wavenumber or eigenvalue
$\delta(x)$	Width of shear layer
ζ	Similarity variable, $(r-h)/b$
η	Radial vortex-sheet displacement
λ	Velocity ratio, U_o/U_i
ρ	Mean density
ω	Angular frequency

Subscripts

a	Ambient flow region
i	Inner flow region
o	Outer flow region

1. INTRODUCTION

The noise generated by aircraft in flight is a major environmental issue. This has forced federal authorities to lay down stringent requirements on the noise generated (FAR-36 Stage III). Jet noise represents a significant percentage of the overall noise generated. This suggests that the reduction of jet noise is of utmost importance to future development of a supersonic civil aircraft. In fact, the environmental regulations require reduction of unsuppressed jet engine noise by 99 percent without suffering any significant thrust loss, see Seiner and Krejsa [1]. Noise reduction strategies, common to all those adopted by the US aircraft industry, involve methods to enhance mixing between two co-flowing streams with different velocity and density ratio's. Most often one stream is subsonic, although there are instances where both are supersonic. Previously, Brown and Roshko [2] have shown, for the two-dimensional mixing layer, that the density ratio between two streams has little effect on mixing in subsonic flow. The criteria for selecting the engine nozzle geometry and stream velocity ratio is that it should (i) minimize the thrust loss, (ii) reduce the extent of supersonic flow region through enhanced mixing, and (iii) shield the noise sources in the inner flow.

The use of coannular jets as a means of reducing jet noise has been studied by several people. Tanna, Tester and Lau [3] were one of the first ones to systematically look at the noise generated by inverted profile coannular jets and compare it to the noise generated by an equivalent single jet, having the same thrust, mass flow rate and exit area as the coannular jet. Based on this comparison, it was shown that the inverted velocity profile is quieter, particularly the low frequency component. The effect of the inverted temperature profile was shown to be insignificant compared to that of the inverted velocity profile. This provided support that the results of Brown and Roshko concerning density ratio also extended into the supersonic regime. Tanna [4] and Tanna and Morris [5] in their work showed that that the normal velocity profile coannular jet is noisier than the equivalent single jet. All these studies involved shock- free conditions and looked at the turbulent mixing noise only. The effect of coannular jets on the shock associated noise was studied by Tanna, Tam and Brown [6]. They concluded that the coannular jet provides the maximum noise reduction relative to the equivalent single jet when the inner (or primary) flow is slightly supersonic, regardless of whether it is an inverted or normal velocity profile. All these suggest that there are some advantages in using

coannular jets, especially, the inverted velocity profile case.

The objectives of this study is to determine theoretically the velocity ratio between two streams that would yield minimum far field generated noise. The streams could both be supersonic or mixed flow (i.e. one stream subsonic) and not necessarily parallel at the initial point of mixing (i.e. nozzle splitter). The inner flow could also contain a solid boundary, such as a nozzle plug. Based on solutions to the compressible Rayleigh model for hot single stream supersonic jets, Seiner, Bhat and Ponton [7] have previously shown that the value of the total growth rate integral and the instability wave phase speed were reliable indicators for determining dominant noise radiated to the far field. From this study it was evident that the shape of the mean velocity profile played a significant role in determining the values of the growth rate integral and wave phase speed. The question of whether an initial dual stream mean velocity profile shape could be found that minimized both the growth rate integral and wave phase speed was a consequence of this previous study.

The initial efforts of finding such a mean velocity profile shape are presented in this report. In order to establish validity to the model, however, requires that it be validated to an existing data base. The normal (NVP) and inverted velocity profile (IVP) jet is a rich source for acoustic data. For example, the IVP acoustic data of Tanna, Tester and Lau [3] show a 3 PNdB noise reduction associated with supersonic streams with a velocity ratio of 1.5. Unlike the experimental study, both the NVP and IVP conditions will be examined theoretically, to establish which profile would lead to lower radiated noise. The study also includes stability calculations for the benchmark equivalent round single jet having the same thrust, mass flow rate and exit area as the NVP and IVP jets. In all cases, the flows are assumed to be shock-free, so that the noise is dominated by the Mach wave emission process.

The eddy Mach wave mechanism, first analytically described by Philips [8], exists only when the turbulence is convected supersonically with respect to the ambient speed of sound. Theoretical predictions have also been made by Ffowcs Williams [9, 10] based on the Lighthill's acoustic analogy approach. However, this approach is fully non-linear requiring extensive computing power. The approach used here is based on the inviscid, linear instability wave model of Tam and Burton [11]. This method is much simpler and easy to implement and has been applied successfully in predicting the noise generated by high temperature supersonic jets, see Seiner, Bhat and Ponton [7]. In this approach, the Mach wave emission process

is modeled as the noise generated by the large-scale turbulent structures (which are considered as superposition of instability waves) in the mixing region. The local characteristics and the axial development of the large-scale structures are determined through the solution of the compressible Rayleigh's equation.

Stability calculations are carried out for a Strouhal number ($St = 2fR_i/U_i$) equal to 0.2 and different spatial modes of importance. This Strouhal number is selected since, from previous studies with single round jets [7], it contains significant acoustic energy in the far field. Also based on these previous studies [7], axisymmetric mode ($n = 0$) and helical modes ($n = 1$ and 2) are found to be generally most significant. In Sec. 2, two models for the instability waves are described. At the jet exit, the simpler vortex-sheet model is used to provide a good estimate of the wavenumber for the more realistic finite thickness shear layer model. The numerical scheme used in solving the Rayleigh's equation is then described. In Sec. 3, numerical results obtained for the different cases are presented and finally, in Sec. 4, a summary of the results is given and also ways of improving the model and plans for future work are discussed.

2. ANALYSIS AND COMPUTATIONAL PROCEDURE

In this section, the equation governing the development of the instability waves is given. The analysis and the numerical schemes are discussed for two different models, i.e., a vortex-sheet model as well as a more realistic model with continuous velocity profile and finite shear layer thickness. The simpler vortex-sheet model provides a good estimate of the phase velocity of an instability wave. However, for an accurate determination of the growth rate of the wave, the finite thickness mixing layer model has to be used. The vortex-sheet model also provides a good initial estimate of the wavenumber for the finite thickness model.

2.1 Vortex-Sheet Model

Consider a coannular jet bounded by vortex-sheets as shown in Fig. 2.1. It is assumed that the ambient air is static. The inner flow (denoted by subscript i) has a velocity U_i and radius R_i and the corresponding values for the outer flow (denoted by subscript o) are U_o and R_o. A cylindrical coordinate system, (r, θ, x), is used as shown in Fig. 2.1 with the x-axis in the flow direction. Using the linearized continuity, momentum and energy equations, it can be shown that the perturbed pressures are governed by

$$\left[\frac{\partial}{\partial t} + U_i \frac{\partial}{\partial x}\right]^2 p_i - C_i^2 \nabla^2 p_i = 0 \qquad (r \leq R_i) \tag{2.1}$$

$$\left[\frac{\partial}{\partial t} + U_o \frac{\partial}{\partial x}\right]^2 p_o - C_o^2 \nabla^2 p_o = 0 \qquad (R_i \leq r \leq R_o) \tag{2.2}$$

$$\frac{\partial^2 p_a}{\partial t^2} - C_a^2 \nabla^2 p_a = 0 \qquad (r \geq R_o) \tag{2.3}$$

where ∇^2 is the Laplacian operator, C_i, C_o and C_a are the speeds of sound in the inner, outer and ambient flow regions and the pressure disturbances in these regions are represented by p_i, p_o and p_a, respectively. The equations are non-dimensionalized with respect to U_i, ρ_i and R_i. The radial displacements of the inner and outer vortex-sheets are given by $\eta_i(\theta, x, t)$ and $eta_o(\theta, x, t)$, respectively. The dynamic and kinematic boundary conditions at $r = R_i$ are

$$p_i = p_o \tag{2.4}$$

$$-\frac{1}{\rho_i}\frac{\partial p_i}{\partial r} = \left[\frac{\partial}{\partial t} + U_i\frac{\partial}{\partial x}\right]^2 \eta_i \tag{2.5}$$

and

$$-\frac{1}{\rho_o}\frac{\partial p_o}{\partial r} = \left[\frac{\partial}{\partial t} + U_o\frac{\partial}{\partial x}\right]^2 \eta_i \tag{2.6}$$

The conditions to be satisfied at $r = R_o$ are

$$p_o = p_a \tag{2.7}$$

$$-\frac{1}{\rho_o}\frac{\partial p_o}{\partial r} = \left[\frac{\partial}{\partial t} + U_o\frac{\partial}{\partial x}\right]^2 \eta_o \tag{2.8}$$

and

$$-\frac{1}{\rho_a}\frac{\partial p_a}{\partial r} = \frac{\partial^2 \eta_o}{\partial t^2} \tag{2.9}$$

The perturbation pressure and the radial displacement are assumed to take the form

$$p(r,\theta,x,t) = \hat{p}(r)\exp\left[i(\alpha x + n\theta - \omega t)\right] \tag{2.10}$$

$$\eta(\theta,x,t) = \hat{\eta}\,\exp\left[i(\alpha x + n\theta - \omega t)\right] \tag{2.11}$$

where α is the axial wavenumber, ω is the angular frequency and n is the azimuthal mode number. Using the form given by Eq. (2.10), it is straightforward to show that the solutions of Eqs. (2.1-2.3) satisfying the boundedness conditions at $r = 0$ and $r \to \infty$ are,

$$\hat{p}_i(r) = A_n J_n(k_i r) \tag{2.12}$$

$$\hat{p}_o(r) = B_n J_n(k_o r) + C_n Y_n(k_o r) \tag{2.13}$$

and

$$\hat{p}_a(r) = D_n H_n(k_a r) \tag{2.14}$$

where

$$k_i = \left[(\omega - \alpha U_i)^2/C_i^2 - \alpha^2\right]^{1/2}$$

$$k_o = \left[(\omega - \alpha U_o)^2/C_o^2 - \alpha^2\right]^{1/2}$$

$$k_a = \left[\omega^2/C_a^2 - \alpha^2\right]^{1/2}$$

Here J_n and Y_n are the Bessel's functions of the first and second kind of order n, respectively and H_n is the Hankel function of the first kind of order n. The

quantities A_n, B_n, C_n and D_n are the unknown coefficients. The dispersion relationship between the wavenumber and angular frequency can be obtained by using Eqs. (2.4-2.9) and is given by

$$D(\omega, \alpha) = M_1 M_2 - M_3 M_4 = 0 \tag{2.15}$$

where

$$M_1 = \frac{k_o}{\rho_o \Omega_o^2} Y_n'(k_o R_i) - \frac{k_i}{\rho_i \Omega_i^2} \frac{J_n'(k_i R_i)}{J_n(k_i R_i)} Y_n(k_o R_i) \tag{2.16}$$

$$M_2 = \frac{k_o}{\rho_o \Omega_o^2} J_n'(k_o R_o) - \frac{k_a}{\rho_a \omega^2} \frac{H_n'(k_a R_o)}{H_n(k_a R_o)} J_n(k_o R_o) \tag{2.17}$$

$$M_3 = \frac{k_i}{\rho_i \Omega_i^2} \frac{J_n'(k_i R_i)}{J_n(k_i R_i)} J_n(k_o R_i) - \frac{k_o}{\rho_o \Omega_o^2} J_n'(k_o R_i) \tag{2.18}$$

$$M_4 = \frac{k_a}{\rho_a \omega^2} \frac{H_n'(k_a R_o)}{H_n(k_a R_o)} Y_n(k_o R_o) - \frac{k_o}{\rho_o \Omega_o^2} Y_n'(k_o R_o) \tag{2.19}$$

$\Omega_i = \omega - \alpha U_i$, $\Omega_o = \omega - \alpha U_o$ and the primes denote derivatives. For a given frequency, ω, the wavenumber, α, is given by the roots of Eq. (2.15). In the next section, the details of the finite thickness shear layer model are presented.

2.2 Finite Thickness Shear Layer Model

Consider the coannular jet flow field shown schematically in Fig. 2.2. The flow field can be divided into four regions: (i) the inner core region, where the mean flow properties are uniform, (ii) the inner mixing region which separates the inner and outer core regions, (iii) the outer core region, and (iv) the outer mixing region which separates the outer core region from the ambient fluid. The linearized equations of motion for an inviscid, compressible fluid together with the instability wave theory can be reduced to the Rayleigh's equation for the perturbation pressure which is given by

$$\frac{\partial^2 \hat{p}}{\partial r^2} + \frac{\partial \hat{p}}{\partial r} \left[\frac{2\alpha}{\Omega} \frac{\partial U}{\partial r} + \frac{1}{r} - \frac{1}{\rho} \frac{\partial \rho}{\partial r} \right] + \beta^2 \hat{p} = 0 \tag{2.20}$$

where $\Omega = \omega - \alpha U$ and $\beta^2 = \rho M_i^2 \Omega^2 - n^2/r^2 - \alpha^2$. Here U and ρ are the mean axial velocity and density, respectively and M_i is the Mach number of the inner flow. All the variables have been non-dimensionalized with respect to the variables of the inner flow. Equation (2.20) governs the axial development of an instability wave of a given real frequency, ω, azimuthal mode number, n, and α, the axial wavenumber,

is the unknown eigenvalue of the problem. Once again, a cylindrical coordinate system, (r, θ, x) is chosen with the jet axis in the x-direction. It is assumed that the flow is locally parallel and that the fluctuating pressure takes the form given by Eq. (2.10).

The eigenvalue can be determined by integrating Rayleigh's equation numerically. The integration can be carried out once the mean velocity and density profiles are defined. It is assumed that the mean velocity can be closely approximated by a half-Gaussian profile. The velocity profile for the inner shear layer is given by

$$U_i(r) = \lambda + (1 - \lambda) f(\zeta_i) \tag{2.21}$$

and for the outer shear layer by

$$U_o(r) = \lambda f(\zeta_o) \tag{2.22}$$

where $\lambda = U_o/U_i$, is the velocity ratio and

$$f(\zeta) = \exp\left[-\ln(2)\ \zeta^2\right], \quad \zeta = \frac{(r-h)}{b} \tag{2.23}$$

In Eq. (2.23), h is the radius of the uniform core region and b is the half-width of the mixing layer. The mean density is related to the mean velocity by the Crocco's relation.

In regions of constant mean flow properties, i.e., the inner and outer core regions and the ambient region, Eq. (2.20) can be solved analytically for the perturbation pressure. These solutions which satisfy the boundedness conditions at $r = 0$ and $r \to \infty$ are

$$\hat{p}_i(r) = A_n J_n(\beta_i r) \tag{2.24}$$

$$\hat{p}_o(r) = B_n J_n(\beta_o r) + C_n Y_n(\beta_o r) \tag{2.25}$$

and

$$\hat{p}_a(r) = D_n H_n(\beta_a r) \tag{2.26}$$

where

$$\beta_i = \left[M_i^2(\omega - \alpha)^2 - \alpha^2\right]^{1/2}$$

$$\beta_o = \left[M_i^2 \rho_o(\omega - \alpha\lambda)^2 - \alpha^2\right]^{1/2}$$

$$\beta_a = \left[M_i^2 \rho_a \omega^2 - \alpha^2\right]^{1/2}$$

As before, the subscripts i, o and a represent the inner, outer and ambient flow regions. These solutions provide the starting values for the numerical integration. In the next section, the details of the numerical scheme to determine the axial wavenumber are discussed.

2.3 Numerical Scheme

First of all, to calculate the axial development of an instability wave, the axial variation of the core radius and the half-widths for the inner and outer flows have to be defined. Usually, this information is obtained from the measured mean velocity data. Here, both the inner and outer flows are supersonic and we were unable to locate adequate data for this case. So, for present purposes, some assumptions have been made regarding the growth of the shear layers. The growth rate of the shear layer is determined from the Langley curve as a function of convective Mach number, see Bradshaw [12]. It is also assumed that the half-velocity point corresponds to the nozzle lip line. This determines h_i, b_i, h_o and b_o as a function of downstream distance.

As mentioned before, Eq. (2.20) is integrated numerically in the shear layer. The solutions given by Eqs. (2.24-2.26) provide the starting solutions for the integration. Two sets of integrations are carried out. The first integration is started from the outer boundary of the inner core region and is integrated through the inner shear layer to the inner boundary of the outer core region. This solution is matched with the known analytic solution in the outer core region. The matching condition requires that the pressure and its derivative be continuous. The second integration is started at the outer boundary of the outer core region and is integrated through the outer shear layer to the ambient flow region. Once again, the integrated and the known solutions are matched. The matching conditions lead to a system of homogeneous equations for the unknown coefficients, A_n, B_n, C_n and, D_n. For this system of equations to have non-trivial solutions, the determinant of the coefficient matrix should be zero. The axial wavenumbers, α, are obtained in an iterative fashion by finding the zeroes of the determinant using a Newton- Raphson scheme. The initial guess for the wavenumber is obtained from the solution of the vortex-sheet model. The other details of the scheme are not elaborated here and can be found in Tam and Burton [11] and also in Seiner and Bhat [13].

3. NUMERICAL RESULTS

As discussed earlier, the mean velocity profile has to be defined first. The growth rate of the shear layer and from it the potential core radius and the half-velocity point are determined based on the assumptions discussed earlier. Two different cases are considered. The first case is the one with inverted velocity profile (IVP) and the second case is the normal velocity profile (NVP). The values of the flow parameters for these two cases are:

Case I: Ratio of radii, $R_o/R_i = 3.0$, $M_i = M_o = 1.48$, Velocity ratio, $U_o/U_i = 1.91$, Static temperature ratios, $T_o/T_i = 3.65$ and $T_a/T_i = 1.35$.

Case II: Ratio of radii, $R_o/R_i = 3.0$, $M_i = M_o = 1.48$, Velocity ratio, $U_o/U_i = 0.52$, Static temperature ratios, $T_o/T_i = 0.27$ and $T_a/T_i = 0.37$.

The growth of the inner and outer shear layers as calculated from the Langley curve for the two cases are shown in Figs. 3.1 and 3.2. The Langley experimental curve relates the shear layer spread coefficient, C_δ, to the shear layer convective Mach number, M_R, in the potential core region of a jet. If $\delta(x)$ represents the width of the shear layer, then

$$\frac{d\delta}{dx} = C_\delta \frac{|\, U_o - U_i \,|}{(U_o + U_i)}$$

The convective Mach numbers of the inner and outer shear layers are respectively determined from

$$M_{R_i} = \frac{2\,|\, U_o - U_i \,|}{C_o + C_i}, \quad M_{R_o} = \frac{2U_o}{C_o + C_a}$$

Here C_i, C_o and C_a are the speeds of sound in the inner, outer and ambient flow regions, respectively. In both the cases, the calculations have been stopped at the end of either the inner or outer core region. This is due to lack of mean velocity data in the fully developed region. For both the inverted and normal velocity profiles, based on the growth rates, it can be seen that the end of outer core region is reached first. These figures also show that the growth rates are low, which, considering the assumptions made, is not entirely unexpected.

The two characteristics associated with an instability wave that are important for the noise radiated to the far field are the phase velocity and growth rate. The location and emission angle of the jet sound field are determined by the phase velocity and growth rate. The stability calculations, from which the values of these

two quantities can be determined, have been carried out for a Strouhal number of 0.2 and three mode numbers. There are two eigenvalues or wavenumbers for a given frequency and mode number corresponding to the two shear layers. In all the results presented here for the inverted and normal velocity profiles, an eigenvalue is represented by $m = (i, j)$ where i represents the first or second eigenvalue and j corresponds to the mode number (0 for axisymmetric mode, 1 for helical mode and so on). Figures 3.3 and 3.4 show the phase velocity with respect to the ambient speed of sound and the growth rates of the various modes for the case of inverted velocity profile. All the waves have supersonic phase velocities and hence would generate Mach wave radiation. The phase velocities of the waves corresponding to the first eigenvalues are higher than those corresponding to the second eigenvalues. However, the growth rates of the second eigenvalues are higher, to about X/R_i 20.0, beyond which the first set of eigenvalues have slightly higher growth rates. The waves corresponding to the first set of eigenvalues reach their neutral point much further downstream than the second set of waves. Based on our assumptions, the potential core lengths have been calculated to be about $35R_i$ for the outer shear layer and $50R_i$ for the inner shear layer. This stretching of the core regions results in a relatively slow rate of decay of the wave, particularly for the first set of eigenvalues. It can also be seen that, though the helical modes have slower phase velocities, their growth rate is much higher than that corresponding to the axisymmetric mode. All these suggest that the noise radiated will be dominated by the waves corresponding to the second set of eigenvalues, especially the helical modes.

Figures 3.5 and 3.6 show the phase velocities and growth rates for the case of normal velocity profile. The phase velocities of the first set of eigenvalues are much higher than those of the second set of eigenvalues. The waves corresponding to the second set of eigenvalues have subsonic phase velocity and will not contribute to the Mach wave radiation process. Once again, the growth rates of the second eigenvalues are much higher than those corresponding to the first eigenvalues up to X/R_i of about 10.0. As before, the first set of eigenvalues damp out further downstream than the second set. However, there appears to be little difference in phase velocities and growth rates of the second set of eigenvalues for the three modes considered. In this case, the noise generated by the first set of waves will dominate the far field. Comparing the results for the inverted and normal velocity profiles, it can be seen that the growth rates for NVP are higher (almost double for the second

set) than that for IVP. The phase velocities (for the first set of eigenvalues) for NVP are higher than the wave speeds of IVP. This implies that the noise radiated by the coannular jet with NVP could be higher than that with the IVP even in the case with both flows supersonic.

Calculations have also been carried out for the equivalent single jet (ESJ). The physical dimensions and the flow parameters for the single jet have been obtained by keeping the thrust, mass flow rate and the exit area same as that in the coannular jet cases. The parameters so obtained are not very different from those of the coannular jet (for both the normal and inverted velocity profiles). For example, the parameters of the ESJ calculated based on the IVP case are: $R_j/R_i = 3.0$, $U_j/U_i = 1.81$ and $T_j/T_i = 3.28$. However, unlike the coannular jets, there is only one shear layer in the case of ESJ. Even in the case of ESJ, the spread rate of the shear layer is determined from the Langley curve [12]. In both the cases, the non-dimensionalizing variables are kept the same, i.e. the flow parameters of the inner flow of the coannular jet. All the comparisons are made for a Strouhal number of 0.2.

The comparisons of the phase velocities between IVP and the ESJ are shown in Figs. 3.7 and 3.8. The first set of eigenvalues of IVP have higher phase speeds than those of ESJ. Close to the jet exit, the phase velocities of the ESJ are slightly less than that of the second set of eigenvalues of IVP for all the modes considered. However, near the axial location for peak noise emission, which, based on the experimental observations of Troutt and McLaughlin [14] and Seiner, McLaughlin and Liu [15] occurs near the location of each wave's neutral point, the waves corresponding to the ESJ are traveling faster than those corresponding to the IVP jet.

The growth rates are compared in Figs. 3.9 and 3.10. ESJ has much higher growth rate in comparison with the first eigenvalues of the IVP coannular jet. In comparison with the second set of wavenumbers, the waves of the ESJ start off with a higher value than that of the coannular jet. This changes at locations further downstream where the waves of the IVP jet have a slightly higher growth rate. Considering the first set of wavenumbers of IVP and the ESJ, it is not clear as to whether the noise radiated by one is higher than the other. The reason is, even though the growth integrals of ESJ are higher than those of IVP, the waves of IVP are traveling faster. In the case of second eigenvalues of IVP jet, the growth integrals are comparable for the two cases. However, the waves of ESJ are traveling

faster than those of IVP. This suggests that the noise radiated by ESJ would be more than that by IVP jet.

The comparison of the phase velocities between ESJ and NVP jet are shown in Figs. 3.11 and 3.12. The phase speeds of NVP jet (based on the first set of eigenvalues) are much higher than those of ESJ. In fact, the phase velocities of the waves of ESJ are subsonic, except in regions close to the jet exit. However, when compared with the second set of eigenvalues, the phase velocities of the ESJ are higher than that of the waves of the coannular jet. In this case, the waves of NVP jet are traveling subsonically and would not lead to Mach wave radiation. The growth rates are compared in Figs. 3.13 and 3.14. The growth rates of ESJ are much higher when compared with first eigenvalues of NVP jet, but there is no appreciable difference when compared with the second set of eigenvalues of NVP jet. As the waves of ESJ are traveling subsonically, irrespective of the growth rates, the noise radiated by the Mach wave emission process would be higher for the NVP jet. This result is consistent with what was observed earlier [4, 5], both, experimentally and theoretically.

4. DISCUSSION AND CONCLUSIONS

In this study, the compressible Rayleigh's equation is solved to analyze the instability waves or the large-scale structures of coannular jets with both the normal and inverted velocity profiles. These calculations have been performed for a Strouhal number of 0.2 and the first three azimuthal modes of the Kelvin-Helmholtz waves. The important characteristics of the instability waves, i.e., phase velocity and growth rate, are considered. It is seen that in general, the axisymmetric mode has a higher phase velocity than the helical modes. The growth rates, on the other hand, are higher for the helical modes as compared to that of the axisymmetric mode. These observations are similar to that of a single jet and, based on the far field calculations for the single jet, it would seem that the helical modes dominate the noise radiated even in the case of coannular jets. The stability calculations indicate that of the two cases considered, NVP and IVP, the IVP coannular jet would be quieter. These solutions when compared with the calculations for the equivalent single jets, also show trends consistent with past observations. In spite of all this, definite conclusions on the noise radiated by different velocity profiles can only be made when the stability calculations are used to determine the far field noise.

The results presented here are preliminary. This study should be considered more as a feasibility study and not for making actual comparisons of the merits and demerits of different velocity profiles with regard to noise generation. The reason for this is that in the present analysis, the mean velocity profile is assumed to be known from experimental data. However, as mentioned earlier, we were not able to get this information for the case with both inner and outer flows being supersonic. As a result, some very simplifying assumptions were made regarding the spread rate of the shear layers. Unpublished work of Propulsion Aeroacoustics Group (PAG) at NASA Langley indicates that the selected spread rates based on the Langley curve may be significantly conservative when applied to supersonic jets. This curve was established from data taken from the two-dimensional shear layer. For a shock-free Mach 2 axisymmetric jet operating into still air, the PAG has measured a shear layer spread rate of $d\delta/dx = 0.2$. The corresponding value from the Langley curve is 0.085. Thus one would expect that once measured mean velocity profiles were determined for the coannular jet, significantly different values for the instability wave growth rate would be determined.

The analysis could not be extended well past the end of the core regions as the

mean velocity in the fully developed region has to defined. This is the reason for selecting a radius ratio, R_o/R_i, of 3.0, which is higher than the typical values used for coannular jets, so that the end of core region is not close to the jet exit. The analysis, however, predicts some of the merits of using the inverted velocity profile in comparison to the coannular jet with the normal velocity profile. The stability calculations also could not be used to make predictions of the far field noise. This requires that the stability calculations be extended well into the fully developed region to completely determine the growth and decay of an instability wave in order to compute the far field directivity. This is especially true for low frequency waves as they damp out farther downstream than the high frequency components. Here, the calculations were stopped whenever the end of either the inner or outer core regions was reached. However, the analysis can be easily extended into the fully developed region provided the mean velocity is known. A more complete analysis has to be done once the data on the mean velocity profiles become available.

4.1 Future Work

Currently, efforts are under way to compute the mean flowfield of the jets (both supersonic and subsonic) and predict the growth rates of the shear layers using computational fluid dynamics (CFD) techniques. This approach will be used to determine the input required for the stability calculations and noise prediction when the experimental data is not available. The CFD algorithm used here is the CRAFT code, Molvik and Merkle [16] and Sinha et al. [17]. CRAFT solves the 1D/2D/Axi/3D Navier-Stokes equations employing upwind/implicit Roe/Total Variation Diminishing (TVD) techniques in a finite-volume framework. These calculations will enable us to determine the mean velocity and the growth rate of the shear layer more accurately. Furthermore, the stability calculations can be extended beyond the end of the core region and the far field noise radiation can be predicted.

The Rayleigh's equation is a linear model and does not take into account the interaction of the instability waves. The effect of the nonlinear interaction of the waves can be neglected if the amplitude of the disturbances, which initiate the instability waves, near the nozzle exit are small. This assumption may not be valid in all cases. The interaction of these waves can be modeled by performing a nonlinear stability analysis using the parabolized stability equations. The governing equations are parabolized by assuming that the velocity profile, wavelength and

growth rate of the waves vary slowly in the axial direction. This implies that the second derivatives $\partial^2/\partial x^2$ and products of first derivatives $\partial/\partial x$ are small and can be neglected. The second assumption is that the disturbances grow and decay as convected instabilities. This analysis also accounts for non-parallel flows. This approach has been successfully applied for stability of boundary layers by Bertolotti [18], Chang et al. [19], amongst others.

In the analysis presented in this report, there is an unknown initial amplitude (at the jet exit) for each of the instability waves considered. In order to make any quantitative predictions on the far field noise, this unknown quantity has to be determined. This would also help in determining the relative contributions by the individual waves to the overall noise radiated. This information can then be used to selectively amplify (or damp) the wave with the least (or most) contribution to the noise field thereby minimizing the jet noise generated. One possible way of determining this initial amplitude is the stochastic approach suggested by Tam and Chen [20]. In this approach, the instability wave spectrum of the jet is regarded as generated by white noise excitation at the jet exit. The future work would involve implementing this scheme in coannular jets. The other work to be done is to include an external low speed (i.e. $M_f \leq 0.3$) flow field to account for forward flight effects.

REFERENCES

1. Seiner, J. M. and Krejsa, E. A., "Supersonic Jet noise and the High Speed Civil Transport", AIAA Paper 89-2358, July, 1989.
2. Brown, G. L. and Roshko, A., "On Density Effects and Large Structures in Turbulent Mixing Layers", Journal of Fluid Mechanics, Vol. 64, 1974, pp. 775-816.
3. Tanna, H. K., Tester, B. J., and Lau, J. C., "The Noise and Flow Characteristics of Inverted Profile Coannular Jets", NASA CR-158995, February, 1979.
4. Tanna, H. K., "Coannular Jets – Are They Really Quiet and Why?", Journal of Sound and Vibration, Vol. 72, 1980, pp. 97-118.
5. Tanna, H. K. and Morris, P. J., "The Noise from Normal Velocity Profile Coannular Jets", Journal of Sound and Vibration, Vol. 98, 1985, pp. 213-234.
6. Tanna, H. K., Tam, C. K. W., and Brown, W. H., "Shock Associated Noise from Inverted Velocity Profile Coannular Jets", NASA CR-3454, August, 1981.
7. Seiner, J. M., Bhat, T. R. S., and Ponton, M. K., "Mach Wave Emission from a High Temperature Supersonic Jet", AIAA Paper 93-0734, January, 1993.
8. Philips, O. M., "On the Generation of Sound by Supersonic Turbulent Shear Layers", Journal of Fluid Mechanics, Vol. 9, 1960, pp. 1-28.
9. Ffowcs Williams, J. E., "The Noise from Turbulence Convected at High Speed", Philosophical Transactions of Royal Society, London, Ser. A, Vol. 255, No. 1061, 1963, pp. 469-503.
10. Ffowcs Williams, J. E., "The Acoustic Analogy – Thirty Years On", IMA Journal of Applied Mathematics, Vol. 32, 1984, pp. 113-124.
11. Tam, C. K. W. and Burton, D. E., "Sound Generated by Instability Waves of Supersonic Jets. Part I - Two-Dimensional Mixing Layers, Part II - Axisymmetric Jets", Journal of Fluid Mechanics, Vol. 138, 1984, pp. 249-271, 273-295.
12. Bradshaw, P., "Compressibility Effects on Free Shear Layers", 1980-1981 AFOSR-HTTM-Stanford Conference on Complex Turbulent Flows: Comparison and Experiment, Vol. 1, Ed. by Kline, S. J., Cantwell, B. J. and Lilley, G. M., Stanford University Press, Stanford, CA, 1982, pp. 364-368.
13. Seiner, J. M. and Bhat, T. R. S., "Model Problems Associated with the Prediction of Noise by High Speed Shear Layers", Computational Aeroacoustics, Eds. J. C. Hardin and M. Y. Hussaini, Springer-Verlag, 1993.

14. Troutt, T. R. and McLaughlin, D. K., "Experiments on the Flow and Acoustic Properties of a Moderate Reynolds Number Supersonic Jet", Journal of Fluid Mechanics, Vol. 116, 1982, pp. 123-156.

15. Seiner, J. M., McLaughlin, D. K., and Liu, C. H., "Supersonic Jet Noise Generated by Large Scale Instabilities", NASA TP-2072, 1982.

16. Molvik, G. A. and Merkle, C. L., "A Set of Strongly Coupled Upwind Algorithms for Computing Flows in Chemical Nonequilibrium", AIAA Paper No. 89-0199, January, 1989.

17. Sinha, N., Dash, S. M., and Hosangadi, A., "Applications of an Implicit Upwind Navier-Stokes Code, CRAFT, to Steady/Unsteady Reacting, Multi-Phase Flowfields", AIAA Paper No. 92-0837, January, 1992.

18. Bertolotti, F. P., "Linear and Nonlinear Stability of Boundary Layers with Streamwise Varying Properties", Ph.D Dissertation, The Ohio State University, 1991.

19. Chang, Chau-Lyan, Malik, M. R., Erlebacher, G., and Hussaini, M. Y., "Compressible Stability of Growing Boundary Layers Using Parabolized Stability Equations", AIAA Paper No. 91-1636, June, 1991.

20. Tam, C. K. W. and Chen, P., "Turbulent Mixing Noise from Supersonic Jets", AIAA Paper 93-4408, October, 1993.

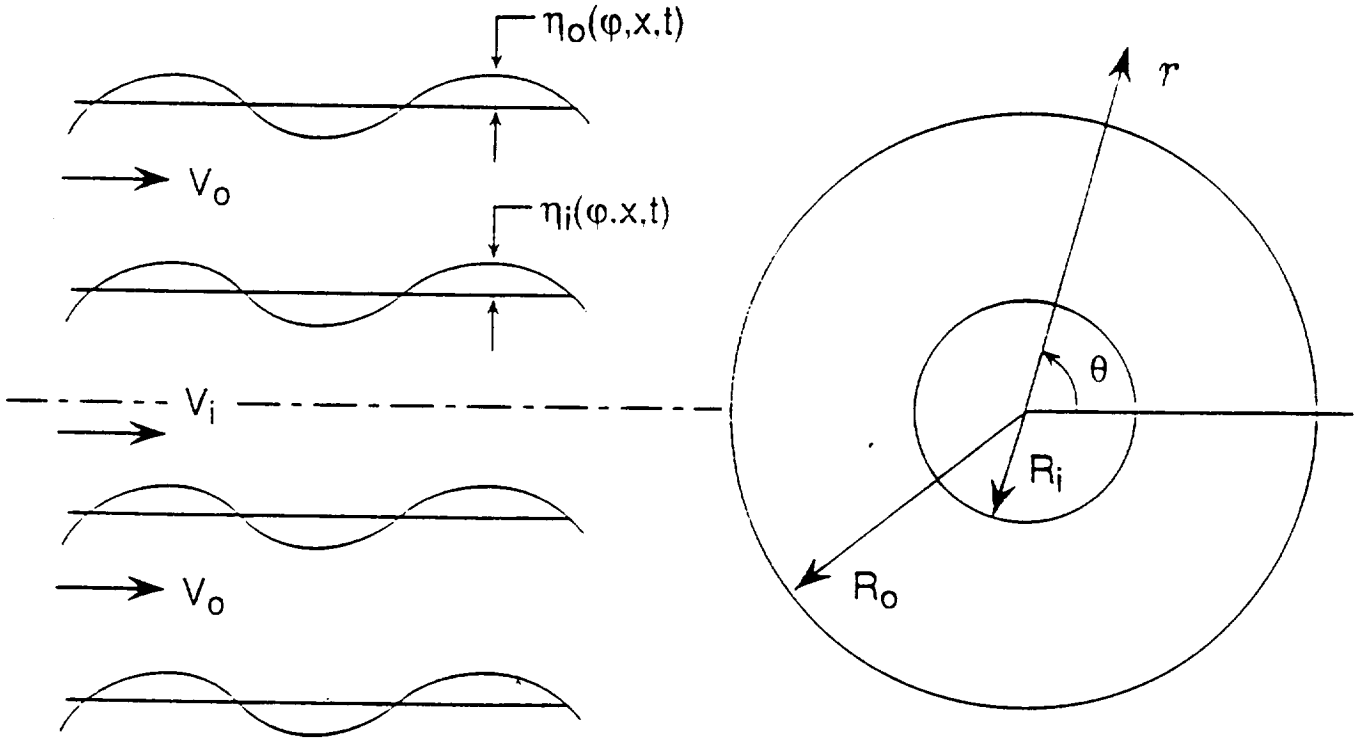

Fig. 2.1 Vortex-sheet model for coannular jet.

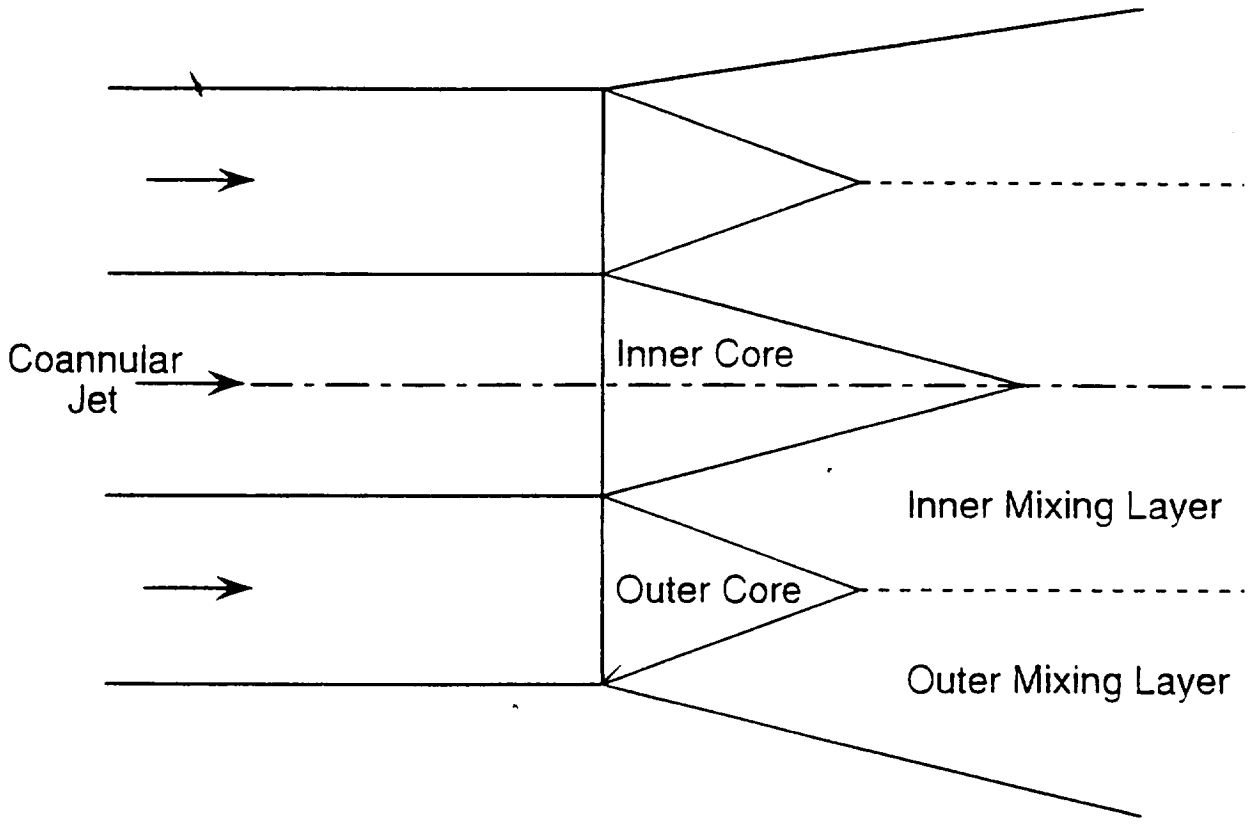

Fig. 2.2 Schematic of a coannular jet flowfield.

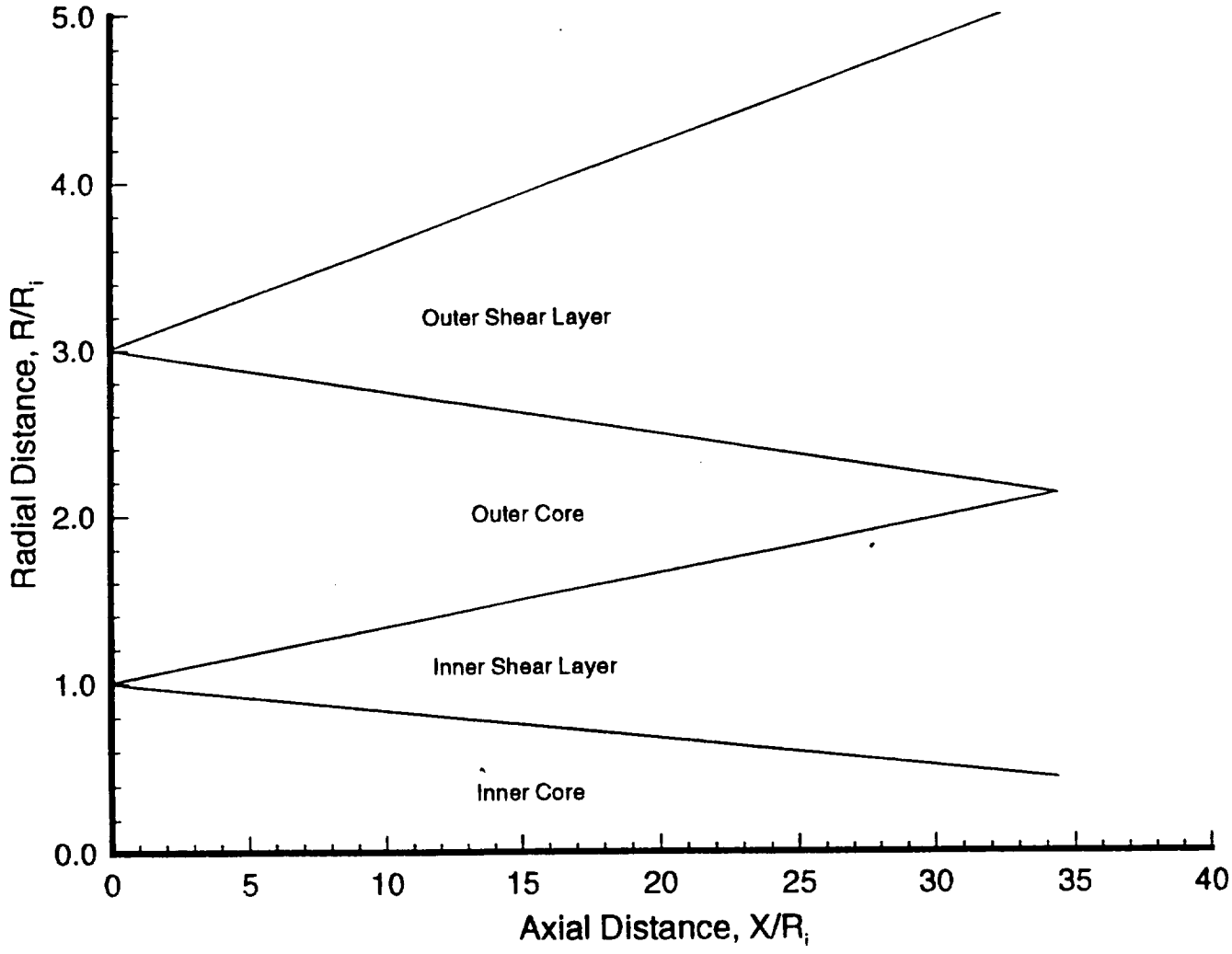

Fig. 3.1 Growth of shear layers for the inverted velocity profile (IVP) coannular jet, case I.

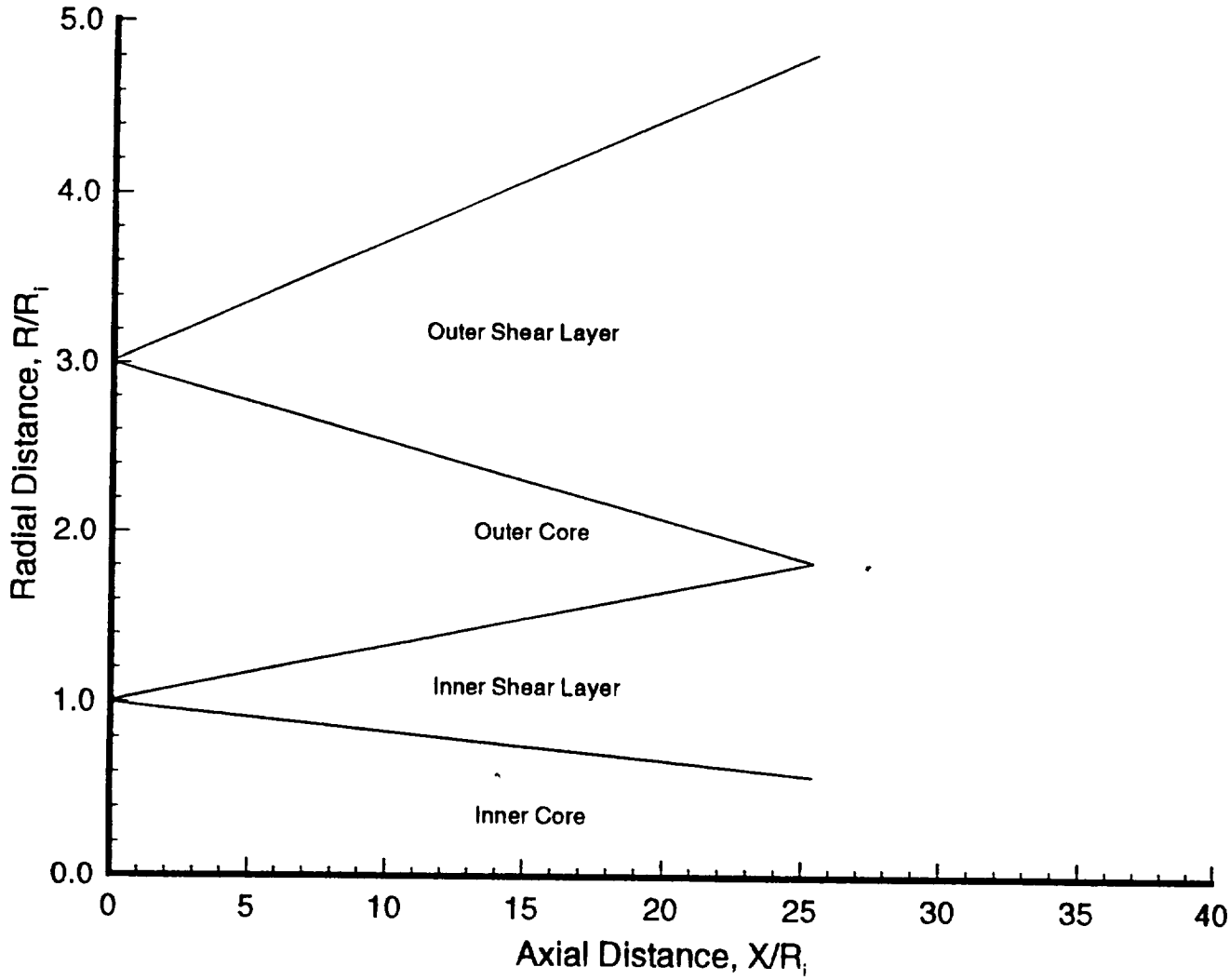

Fig. 3.2 Growth of shear layers for the normal velocity profile (NVP) coannular jet, case II.

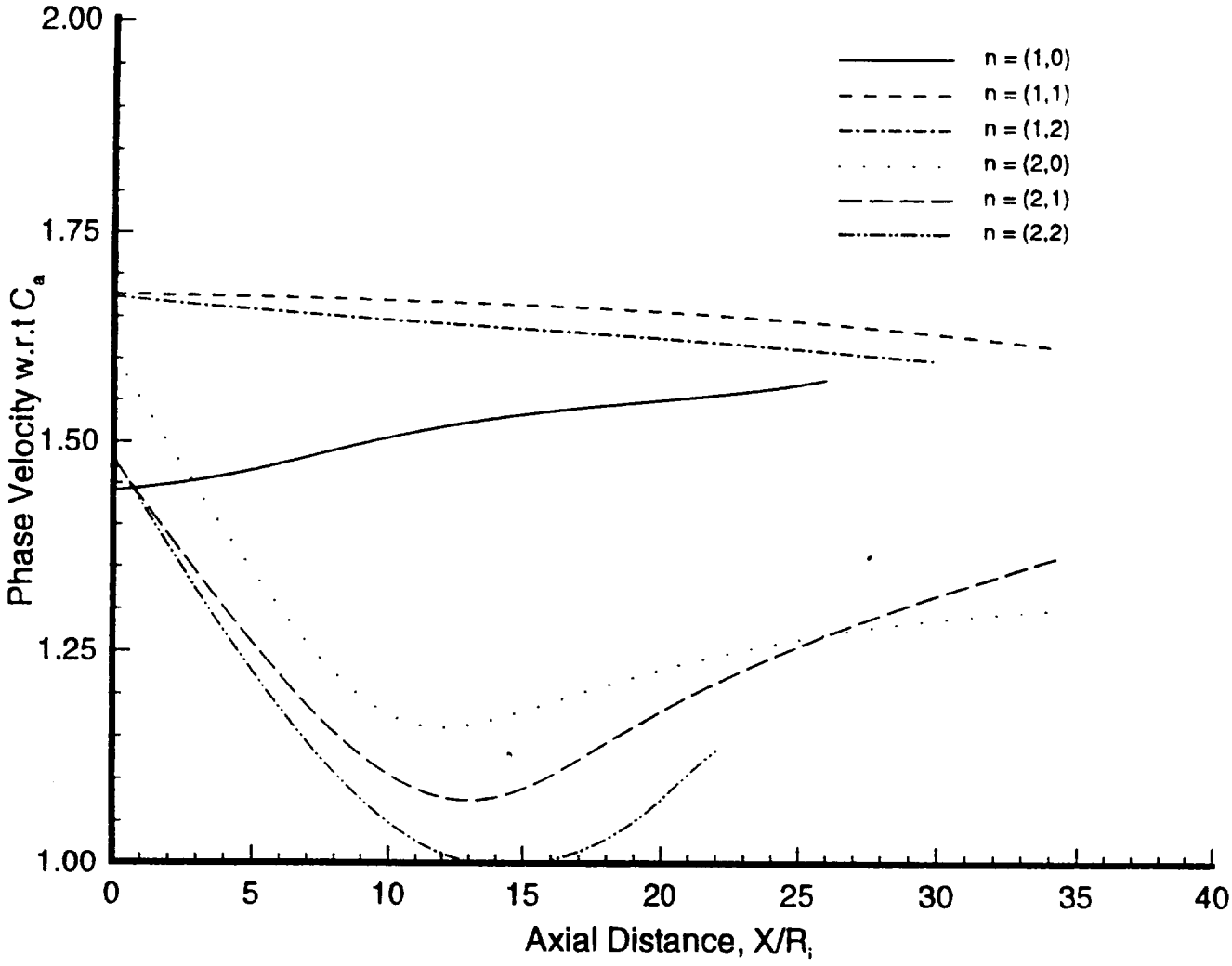

Fig. 3.3 Axial variation of phase velocity, IVP, case I, St=0.2.

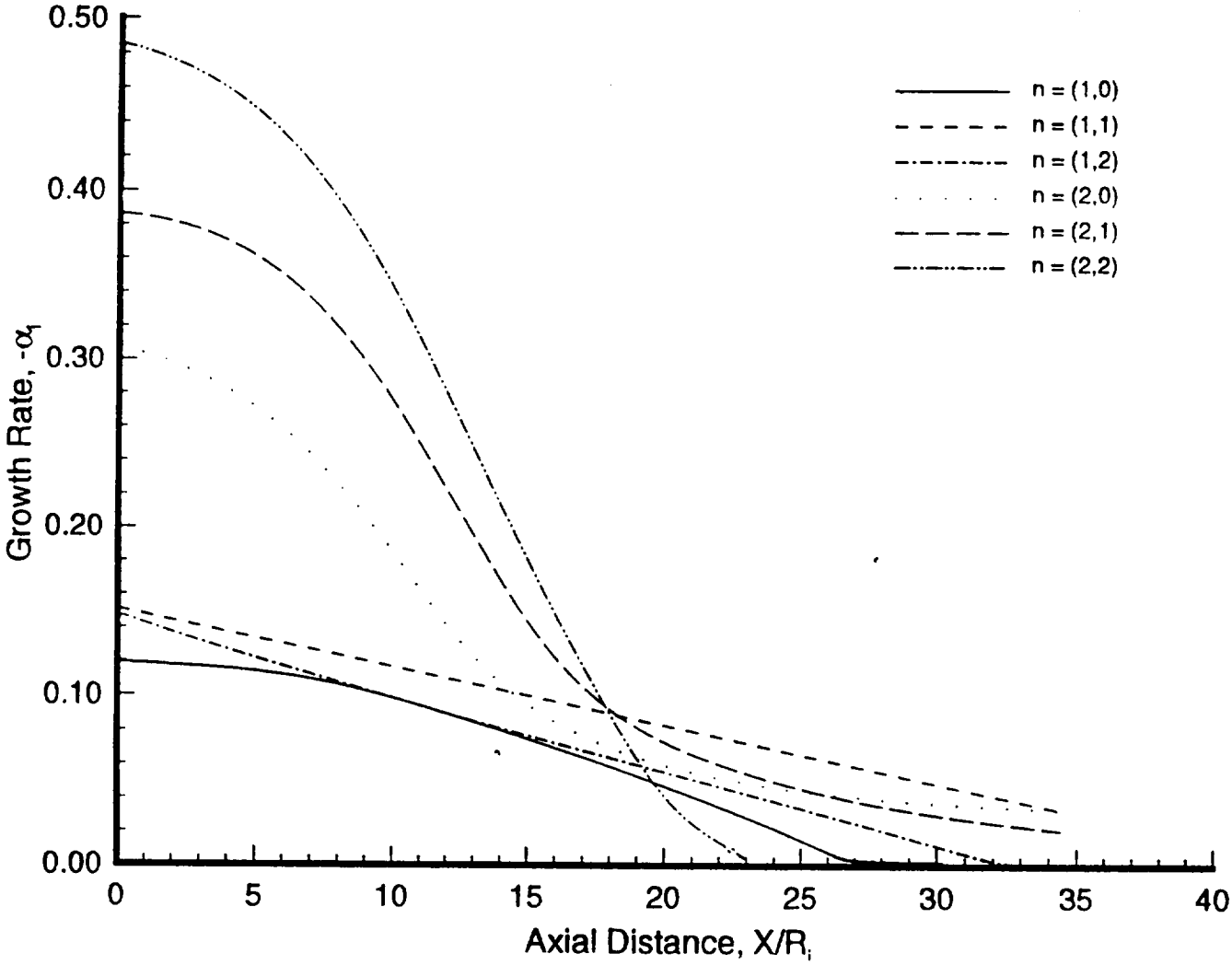

Fig. 3.4 Axial variation of growth rate, IVP, case I, St=0.2.

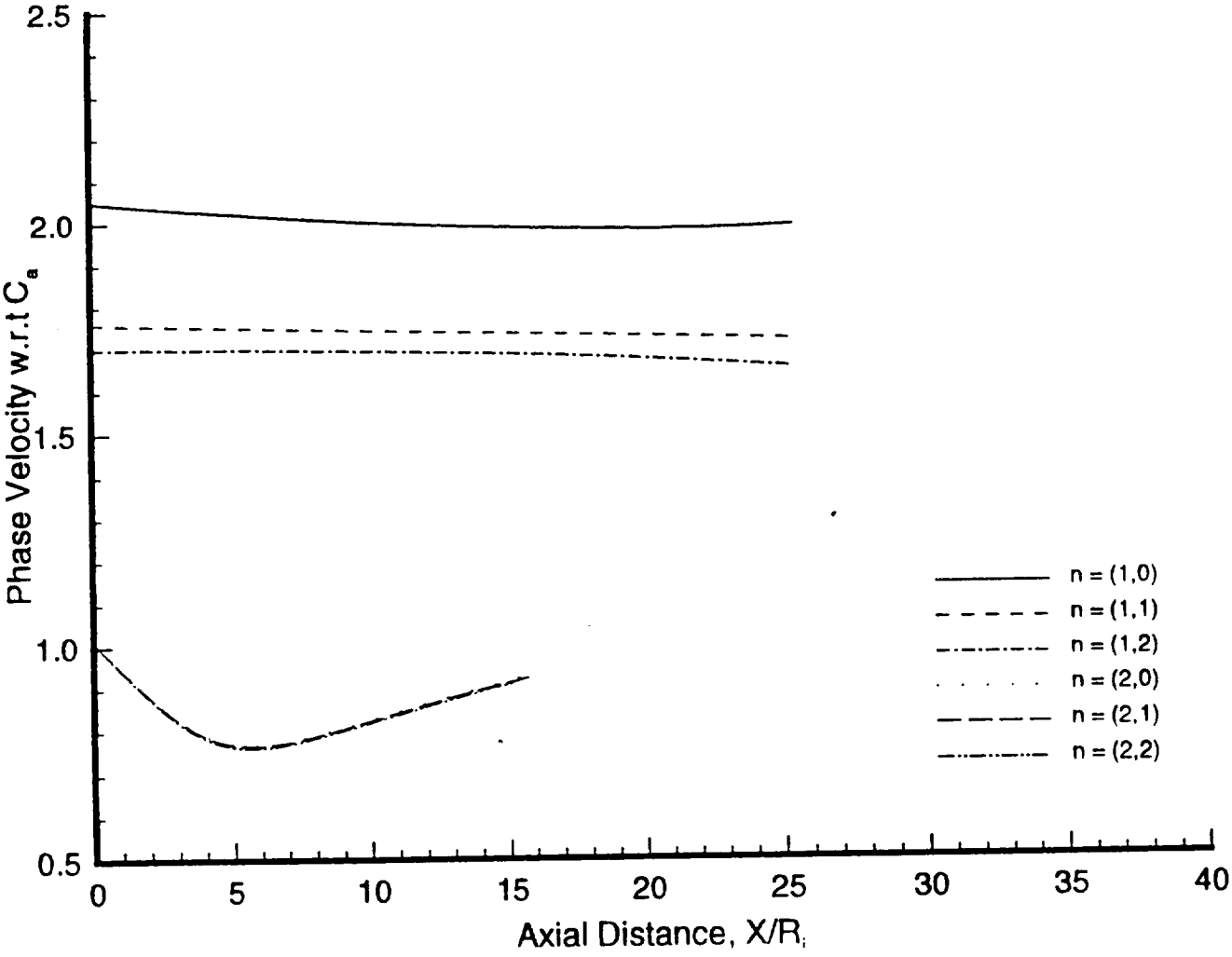

Fig. 3.5 Axial variation of phase velocity, NVP, case II, St=0.2.

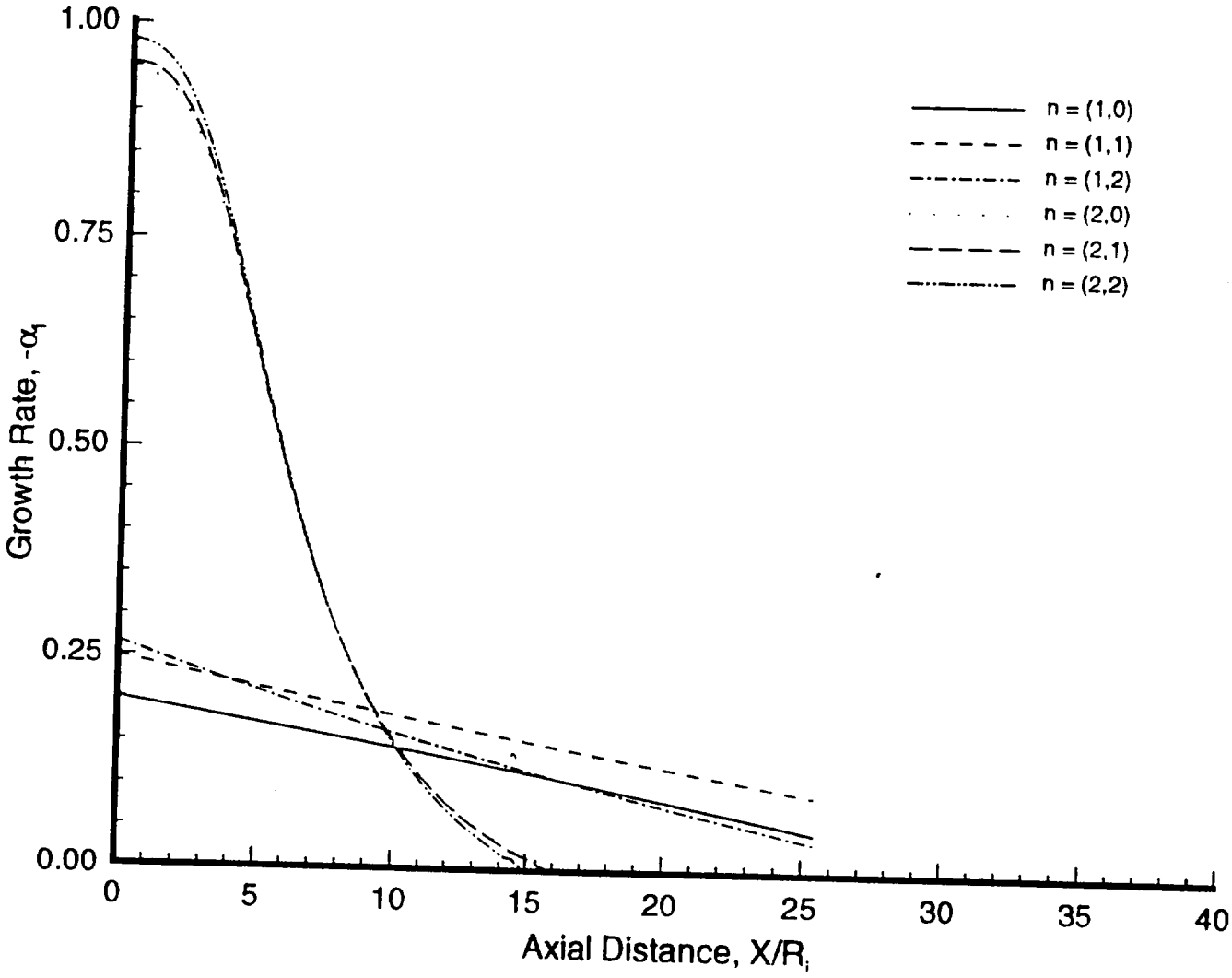

Fig. 3.6 Axial variation of growth rate, NVP, case II, St=0.2.

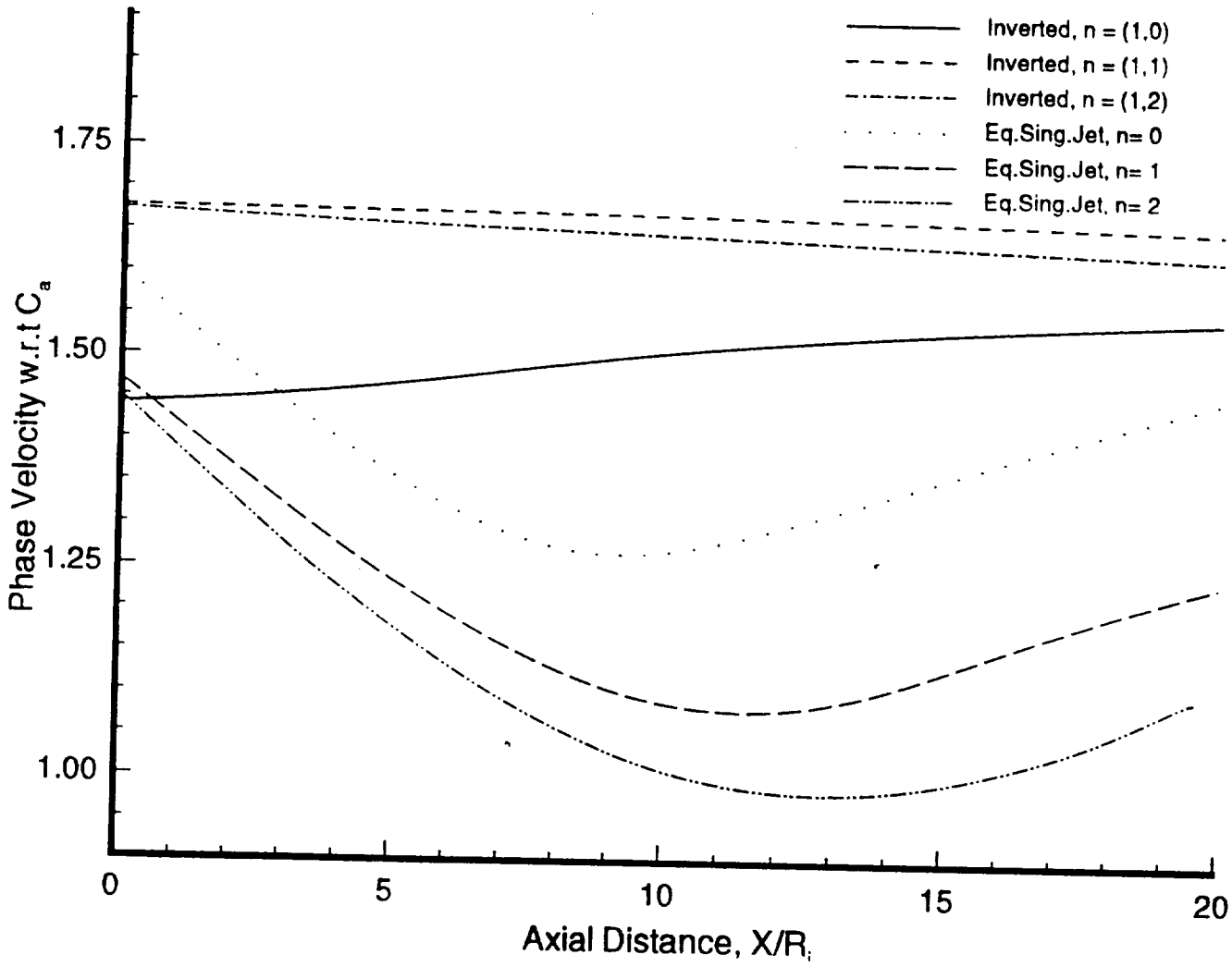

Fig. 3.7 Comparison of phase velocities, IVP (first set of wavenumbers) and equivalent single jet (ESJ), St=0.2.

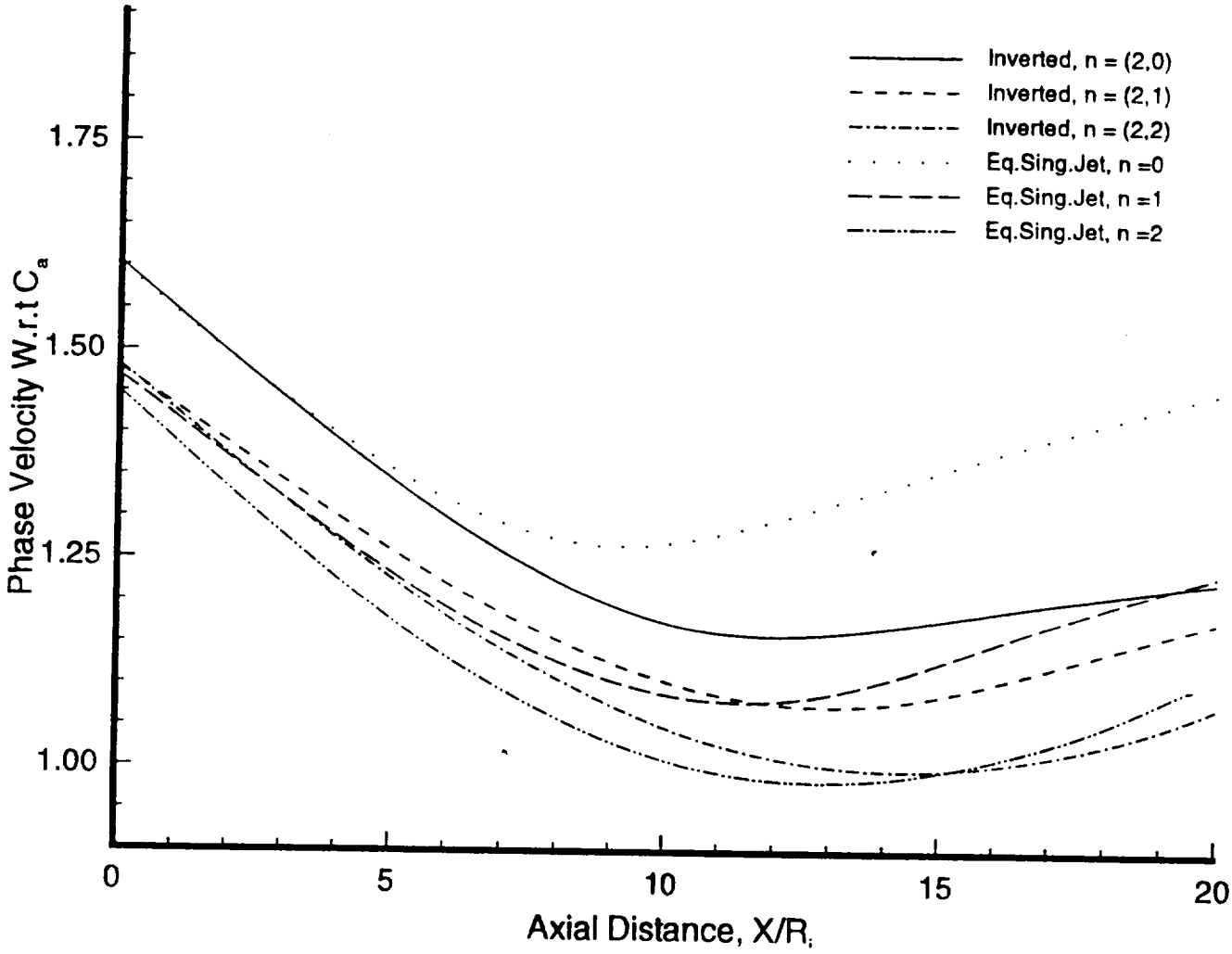

Fig. 3.8 Comparison of phase velocities, IVP (second set of wavenumbers) and ESJ, St=0.2.

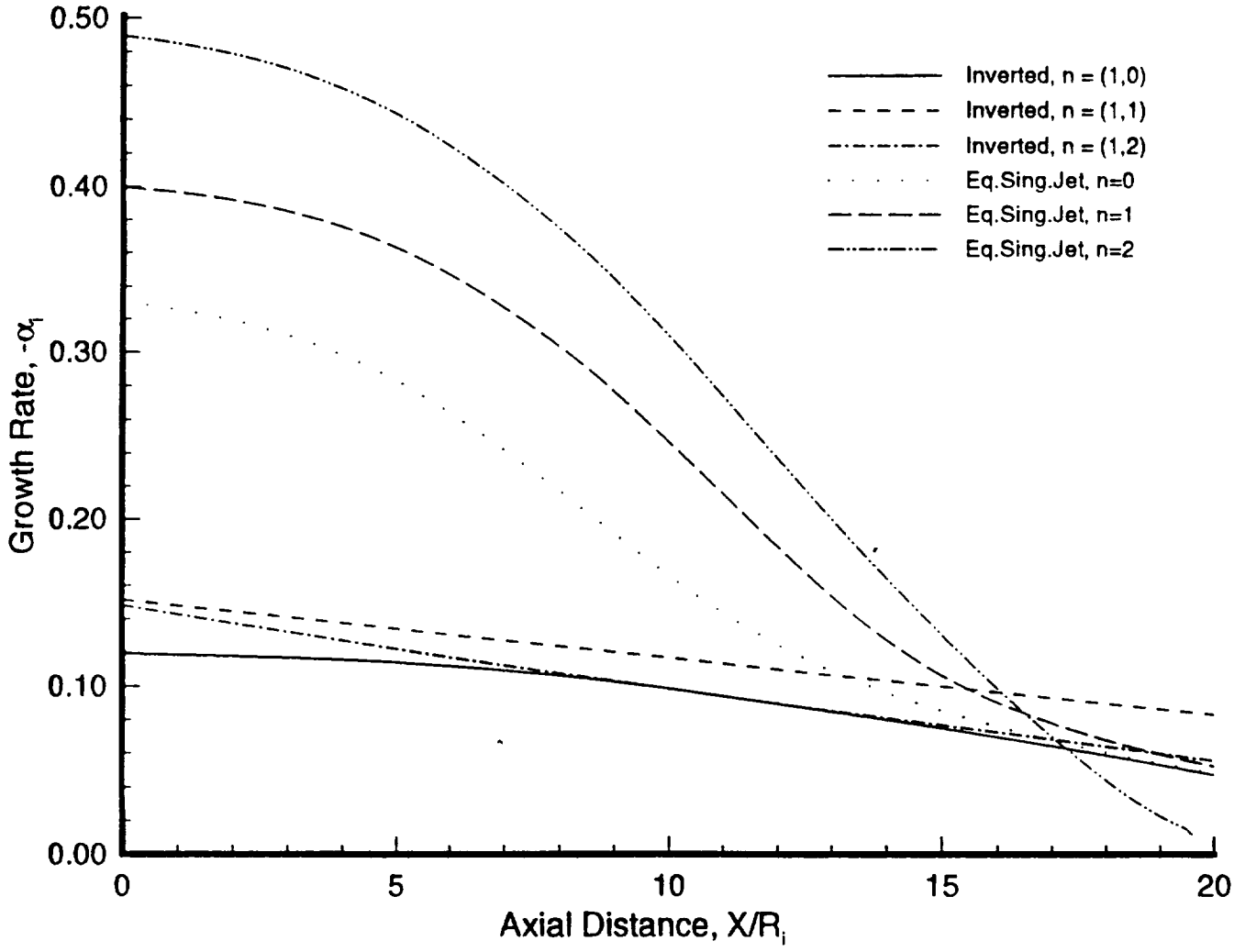

Fig. 3.9 Comparison of growth rates, IVP (first set of wavenumbers) and ESJ, St=0.2.

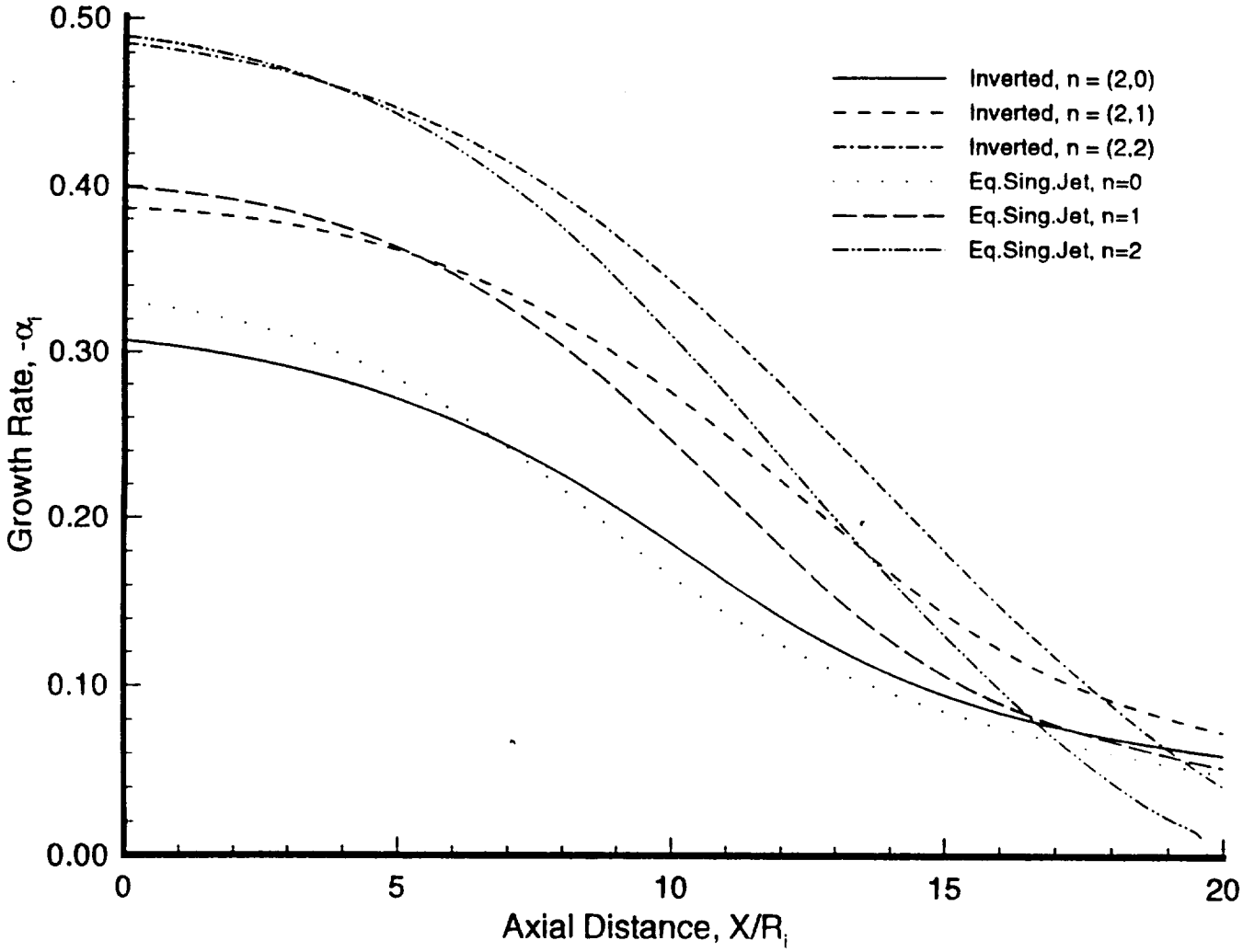

Fig. 3.10 Comparison of growth rates, IVP (second set of wavenumbers) and ESJ, St=0.2.

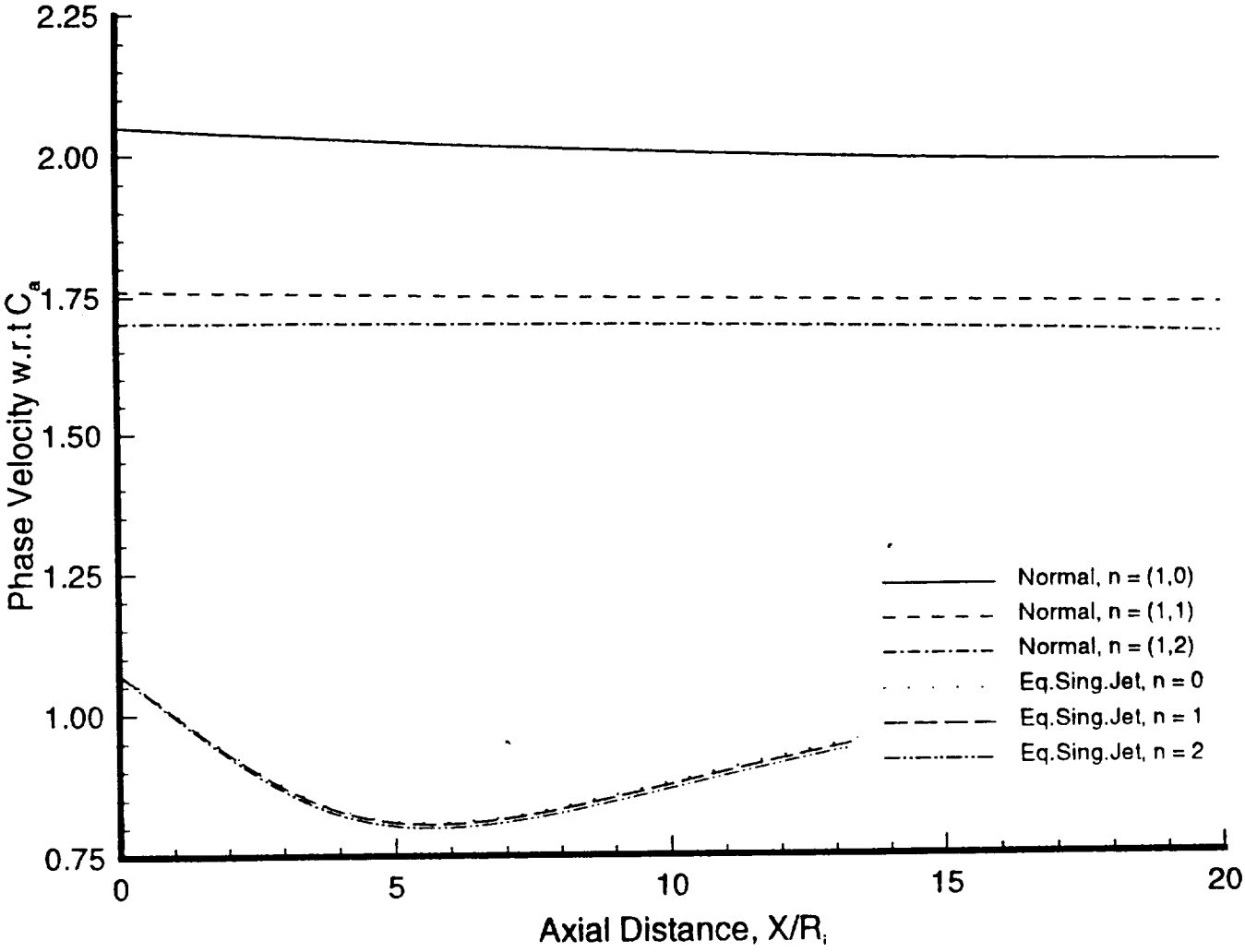

Fig. 3.11 Comparison of phase velocities, NVP (first set of wavenumbers) and ESJ, St=0.2.

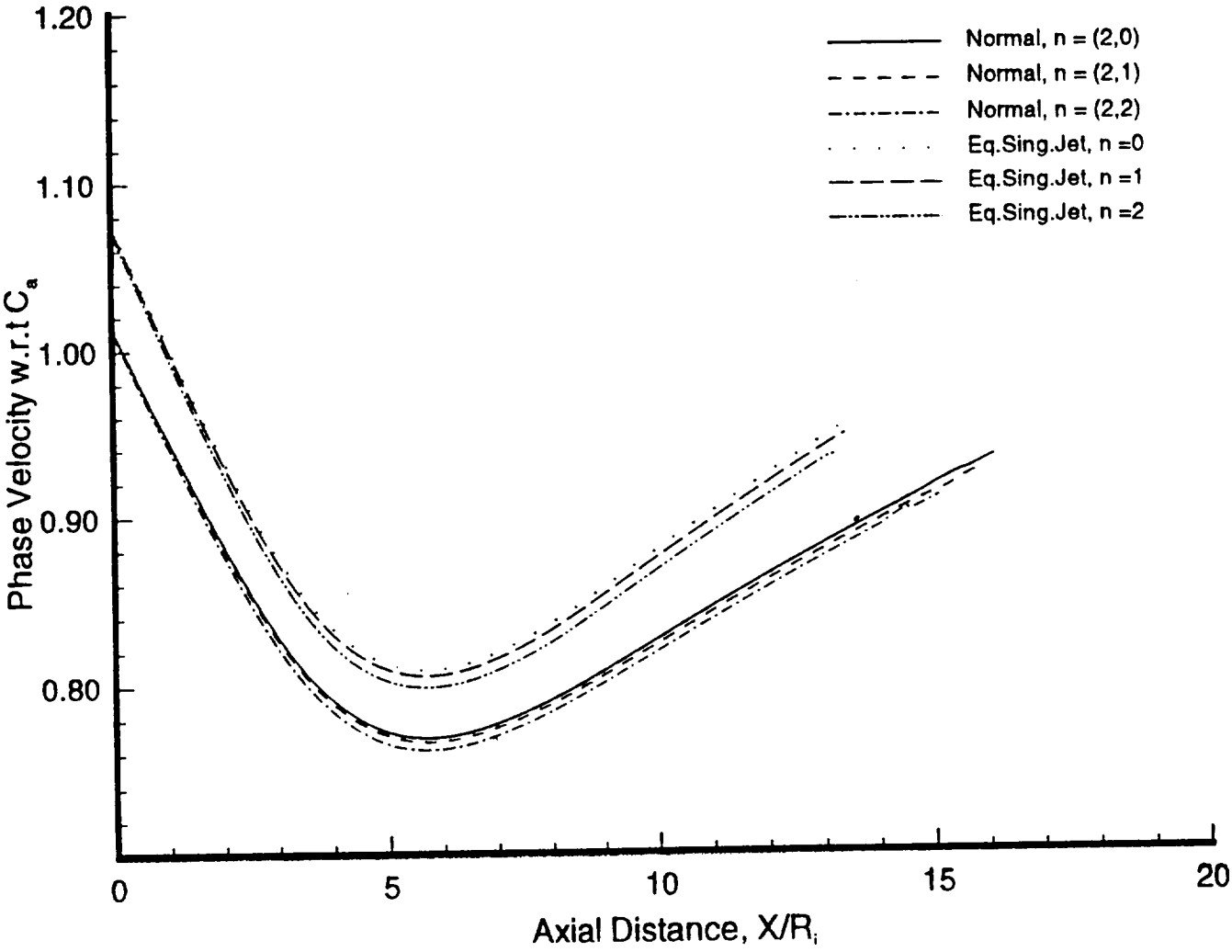

Fig. 3.12 Comparison of phase velocities, NVP (second set of wavenumbers) and ESJ, St=0.2.

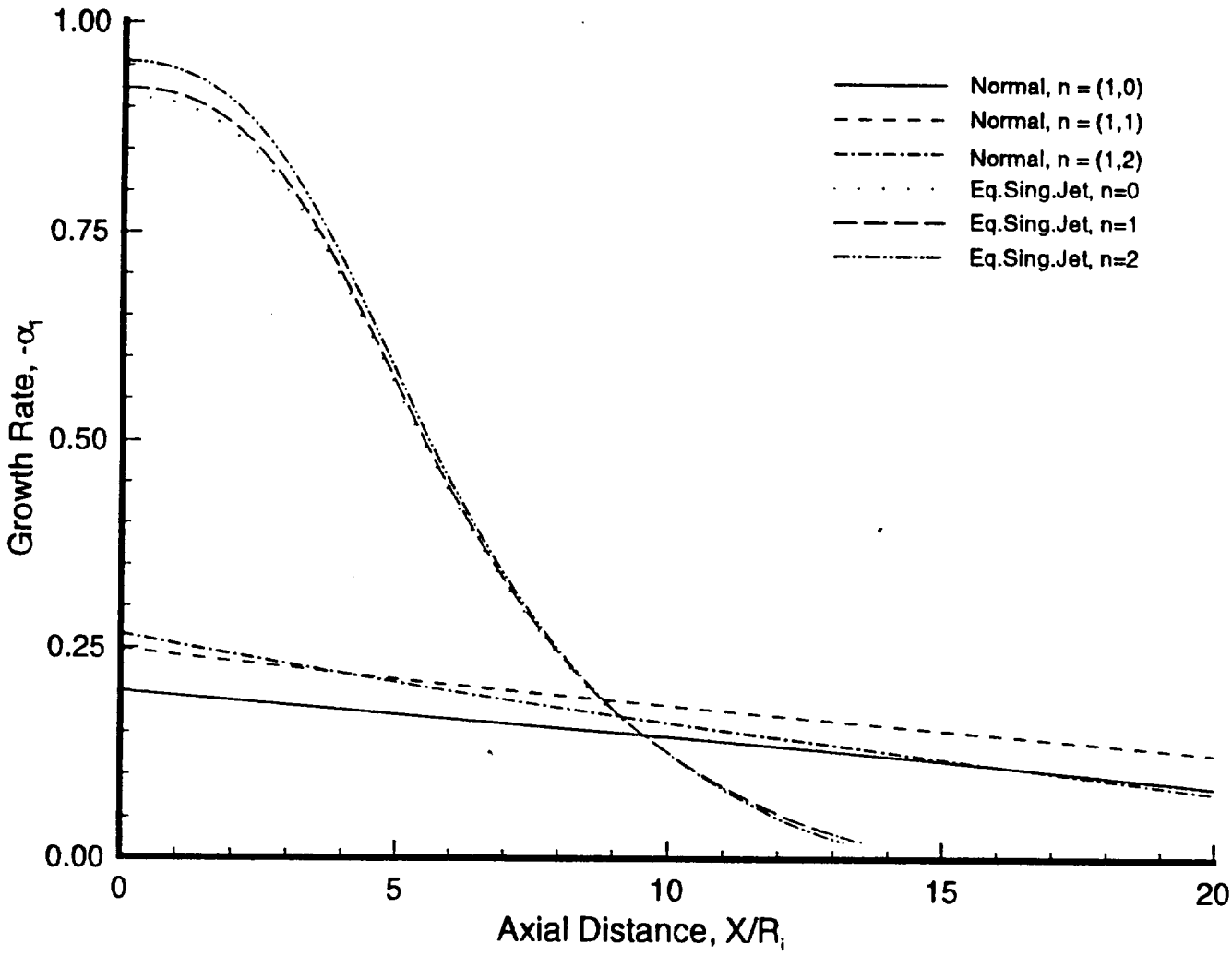

Fig. 3.13 Comparison of growth rates, NVP (first set of wavenumbers) and ESJ, St=0.2.

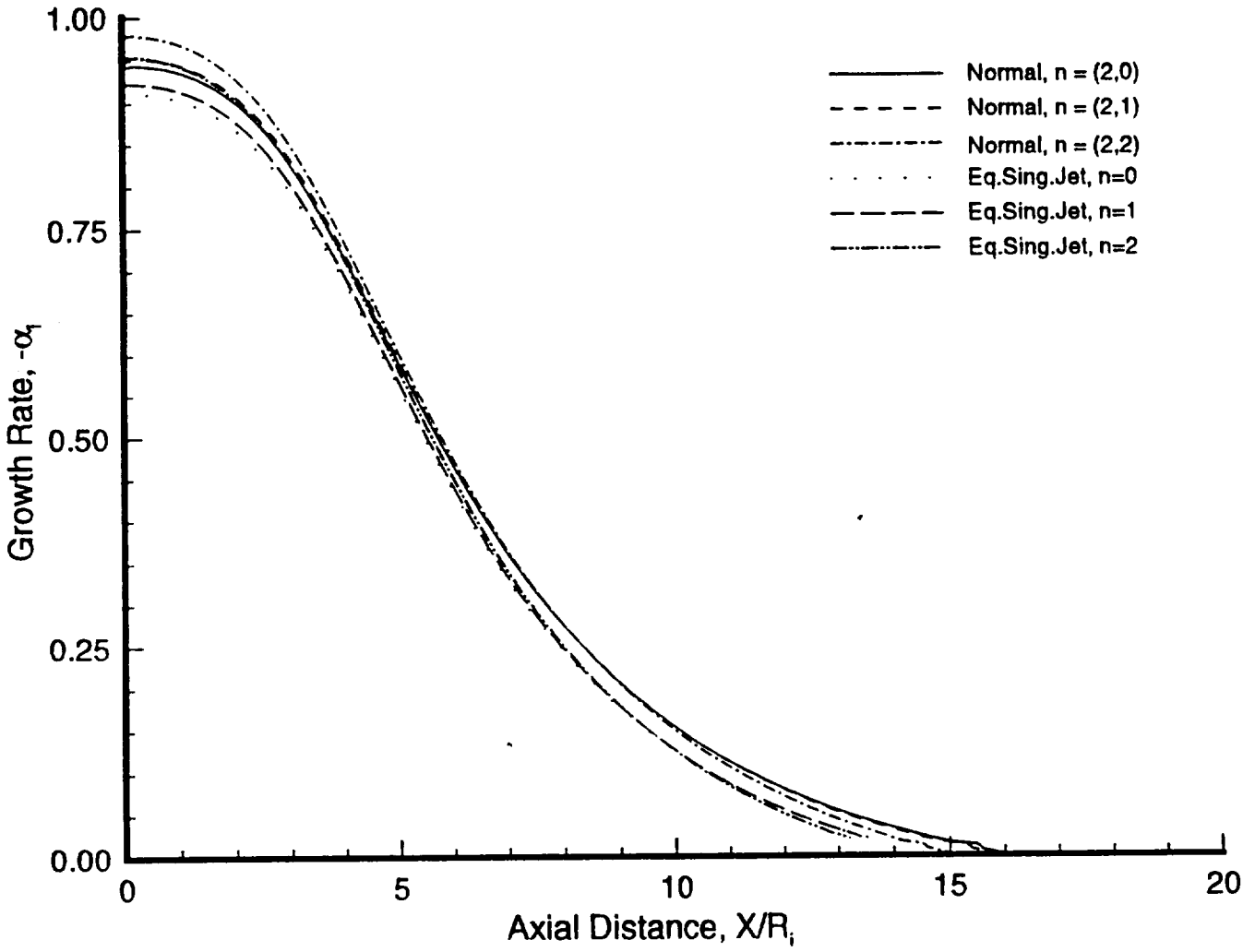

Fig. 3.14 Comparison of growth rates, NVP (second set of wavenumbers) and ESJ, St=0.2.